Chapter 2
Musculoskeletal Robotics Modeling and Simulation

Ahmad Zaki bin Hj Shukor, Fariz bin Ali@Ibrahim, Muhammad Fahmi bin Miskon, Mohd Shakir bin Md Saat and Mohd Khairi bin Mohamed Nor

Abstract This paper presents the kinematics and dynamics of a musculoskeletal model inspired by humans/animals where the bones (links) are actuated by muscles (linear actuators). Starting from a single-link musculoskeletal structure, the kinematics were addressed to link the joint and muscle variables. From the kinematic constraints, dynamics of the structure were also presented. Later the 3D model of a two-link structure was constructed in ROCOS software to simulate the effect of gravity and environment (floor). In the simulations, the constraints were correctly defined as snapshots show the bones and muscle are intact before and after contact with environment.

Keywords Biarticular · Monoarticular · Musculoskeletal · Closed-chain · Redundant

2.1 Introduction

Conventional robotic designs utilize joint actuation using rotational actuators, geared or other transmission mechanism to achieve angular motion that moves arm-like structures [1, 2]. These designs have shown vast applications in industrial

A. Z. bin Hj Shukor (✉) · F. bin Ali@Ibrahim · M. F. bin Miskon
Fakulti Kejuruteraan Elektrik, Universiti Teknikal Malaysia Melaka, Durian Tunggal, Malaysia
e-mail: zaki@utem.edu.my

M. S. bin Md Saat
Fakulti Kejuruteraan Elektronik, Universiti Teknikal Malaysia Melaka, Durian Tunggal, Malaysia

M. K. bin Mohamed Nor
Fakulti Kejuruteraan Mekanikal, Universiti Teknikal Malaysia Melaka, Durian Tunggal, Malaysia

H. A. Mat Sakim and M. T. Mustaffa (eds.), *The 8th International Conference on Robotic, Vision, Signal Processing & Power Applications*,
Lecture Notes in Electrical Engineering 291, DOI: 10.1007/978-981-4585-42-2_2,

robotic arms used in manufacturing such as in spray painting and assembly for cars, as well as mobile/legged robotics in various fields, such as space exploration [3] and concrete pipe inspection [4]. In recent times, robotic structures have also been inspired by the musculoskeletal arrangements of humans/animals. In short, the muscles actuate the motion of the bones/skeleton by extending or contracting, causing joint movement of the arms/legs. Another interesting property of musculoskeletal robotics is the redundant actuation of the muscles which results in improved shape and magnitude of the force ellipsoid of the end effector, for example musculoskeletal biarticular actuation as compared to monoarticular actuation [5].

In terms of muscle actuation, researchers venture into the use of different actuators for implementation. For the four-legged robot HyQ [6], pneumatic cylinders were used in their leg design for flexion motion. Biwi, the wire driven robot arm [7] uses six motors to pull/extend six cables to represent the six muscles from shoulder to elbow. Infinity norm approach was used to distribute forces from the end effector to the six muscles (motors). Another design uses rotational motors with planetary gears to represent redundant actuation of the muscles on the joints [8] and utilize biarticular muscle torque.

2.2 Kinematics of a Musculoskeletal Structure

The musculoskeletal structure in this paper refers to the representation of a muscle with a linear extension/contraction. Consider a single link planar musculoskeletal robotic structure as shown in Fig. 2.1.

The single link (bone) structure is composed of a muscle, rotational joint, and bones. The motion desired is on the bones connected to θ_1, but derived from the extension/contraction of muscle. The angle between the base and muscle, θ_2 also changes with θ_1. However focus is on θ_1 because it is the position where most joint actuators are placed in conventional robotics. The kinematics linking rotational angle θ_1 and muscle length l_1 can be derived from trigonometry (2.1).

$$\begin{aligned} l_1 &= \sqrt{(a_1 + a_2)^2 + (a_3 \sin\theta_1)^2} \\ &= \sqrt{(a_1 + a_3\cos\theta_1)^2 + (a_3 \sin\theta_1)^2} \\ &= \sqrt{a_1^2 + 2a_1a_3\cos\theta_1 + a_3^2} \end{aligned} \tag{2.1}$$

The kinematics is essential to determine the angle from the muscle length and vice versa. This means that a linear actuator equipped with a linear position encoder representing the muscle does not require a joint position encoder to measure the joint angle. A further differentiation of the length with respect to joint angle would result in the Jacobian linking the muscle and joint velocities.

Fig. 2.1 Musculoskeletal single link structure

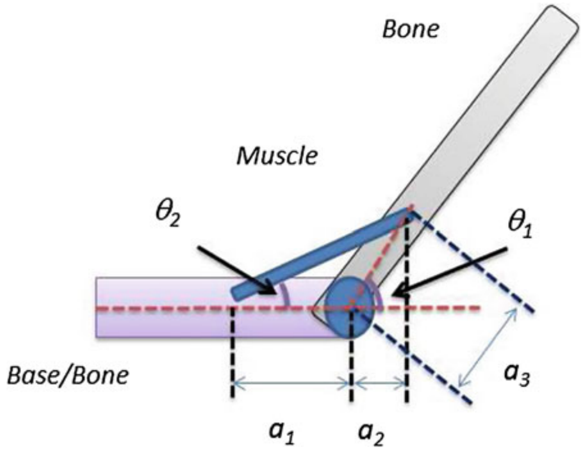

2.3 Dynamics of a Musculoskeletal Structure

A generalized equations of motion of an open-link robotic mechanism can be defined as in (2.2) where τ is the generalized force/torque vector, M is the mass matrix, C is the Centrifugal/Coriolis term and G is the gravity term which could be obtained by any dynamic modeling technique (i.e. Lagrange–Euler, Newton–Euler).

$$\tau = M(\theta)\ddot{\theta} + C(\theta, \dot{\theta})\ddot{\theta} + G(\theta) \tag{2.2}$$

The structure in Fig. 2.1 is not an open-link robot, because there exist a closed-kinematic loop/chain between the muscle and the bone. Thus for a closed-link structure, its dynamics are governed by (2.3) and (2.4):

$$\tau + J_c^T \lambda = M(\theta)\ddot{\theta} + C(\theta, \dot{\theta})\ddot{\theta} + G(\theta) \tag{2.3}$$

$$J_c\ddot{\theta} + \dot{J}_c\dot{\theta} = 0 \tag{2.4}$$

J_c is the Jacobian of the constraint equation (closed kinematics) while λ is the Lagrange multiplier. The term $J_c^T \lambda$ represents the constraint (internal) forces of the muscle loop. As an example, the constraint equations of Fig. 2.1 are depicted as K_1 and K_2 as shown.

$$a_1 + a_3 \cos\theta_1 - l_1 \cos\theta_2 = K_1 = 0 \tag{2.5}$$

$$a_3 \sin\theta_1 - l_1 \sin\theta_2 = K_2 = 0 \tag{2.6}$$

By differentiating the constraint equations with respect to the motion variables of the structure (θ_1, θ_2 and l_1), the following constraint Jacobian (J_c) can be obtained.

$$\begin{bmatrix} \frac{\partial K_1}{\partial \theta_1} & \frac{\partial K_1}{\partial \theta_2} & \frac{\partial K_1}{\partial l_1} \\ \frac{\partial K_2}{\partial \theta_1} & \frac{\partial K_2}{\partial \theta_2} & \frac{\partial K_2}{\partial l_1} \end{bmatrix} = \begin{bmatrix} -a_3 \sin\theta_1 & l_1 \sin(\theta_2) & -\cos\theta_2 \\ a_3 \cos\theta_1 & -l_1 \cos(\theta_2) & -\sin\theta_2 \end{bmatrix} \tag{2.7}$$

The dynamics of the structure stated in (2.3) and (2.4) can also be constructed in matrix form as shown in (2.8).

$$\begin{bmatrix} M & -J_c^T \\ -J_c & 0 \end{bmatrix} \begin{bmatrix} \ddot{\theta} \\ \lambda \end{bmatrix} = \begin{bmatrix} \tau - C\dot{\theta} \\ \dot{J}_c \dot{\theta} \end{bmatrix} \tag{2.8}$$

From the equations of motion of closed-kinematics musculoskeletal structure shown in (2.8), the movement of the structure can be simulated/visualized. Note that the Lagrange multiplier λ also changes with time, along with the generalized accelerations. For simulation of closed-kinematic structure with environmental effects (i.e. floor), the term $J^T F_e$ can be added to (2.3). The term represents the reaction forces of the structure when in contact with the floor.

2.4 Simulation

From the single-link structure shown, two other structures were considered for simulation. This is shown in Fig. 2.2. The simulation software used is the Robot Control Software (ROCOS) developed by Yasutaka Fujimoto at Yokohama National University [9]. Note that the increase in the number of linear actuators incurs redundancy in the biarticular two-link structure. Kinematic equations derived for the biarticular muscle using trigonometry (l_3) shows that the shoulder (θ_1) and elbow joint angles (θ_2) are both present in the muscle equation (2.9).

$$l_3 = \sqrt{a_{31}^2 + a_{32}^2 + a_1^2 + 2a_{31}a_1\cos\theta_1 + 2a_{32}a_1\cos\theta_2 + 2al_{31}al_{32}\cos(\theta_1 + \theta_2)} \tag{2.9}$$

Some of the initial conditions that need to be pre-defined are the link parameters such as mass and length. Other important parameters include the connection length and angles between the muscles and the links (bones). These muscle lengths and joint angles at initial condition must be correctly defined using the muscle-joint kinematics.

Both structures were simulated with the effect of gravity and without any control to demonstrate it falling with gravity (Fig. 2.3). In these conditions, the structure (links and muscle) falls to the floor while the base is static. This shows that the closed-link pre-defined initial conditions (lengths and angles) were set correctly.

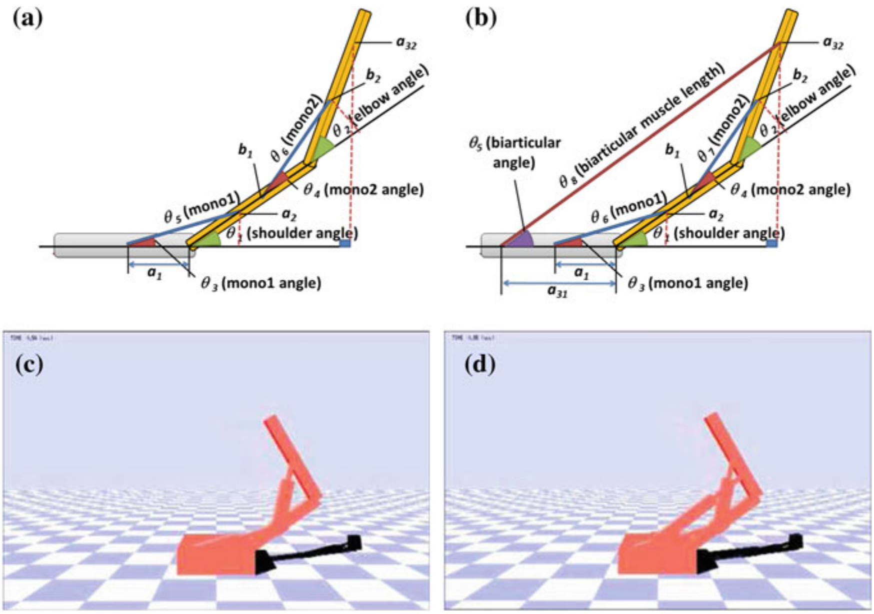

Fig. 2.2 **a** Monoarticular two-link structure. **b** Biarticular two-link structure. **c** Rocos model of (**a**) and **d** Rocos model of (**b**)

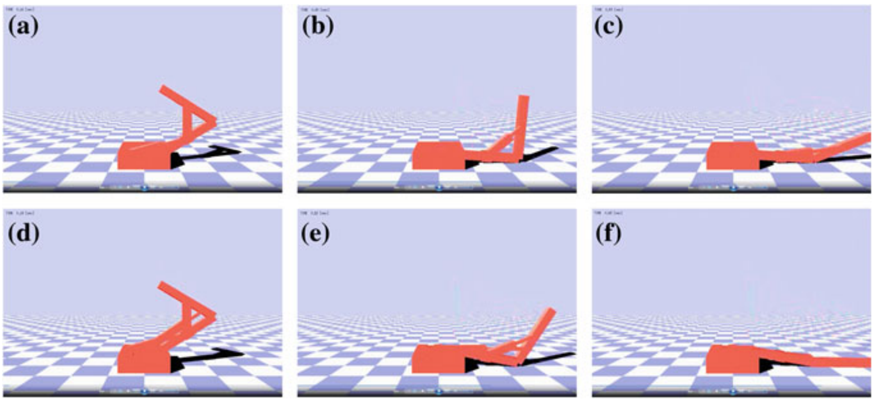

Fig. 2.3 Monoarticular (**a**–**c**) and biarticular (**d**–**f**) structure falling with gravity

2.5 Discussion

At first, the musculoskeletal structure proposed was explained in terms of its kinematic properties. The muscle kinematics relate muscle length and joint angles for motion. Then, the closed-kinematic structure incur a different dynamics representation due to the muscles forming a closed loop within the structure inducing constraint equations and Jacobian. In the simulations, two structures were modeled, one structure with monoarticular (single-joint actuation) muscles and one structure with biarticular (two-joint actuation) muscle. The simulation tests show the success in modeling in ROCOS software because the structures fall with gravity to the floor. The intention of the simulations is to verify the correct definitions of constraints in both monoarticular and biarticular structure and not to compare performance results between the two. Thus the results in this paper are only the snapshots of the models with gravity and environmental effects.

2.6 Conclusion

A new musculoskeletal robotic structure incurs new kinematic and dynamic properties. To model the structure, kinematic relations induces constraints that must be included in the dynamics. A correct definition of kinematic properties would result in successful motion in dynamics simulation software. The success in modeling in software would induce further work which includes application of muscle position and force control on the musculoskeletal structure to explore the advantages of redundant actuation.

Acknowledgments Authors wish to acknowledge Universiti Teknikal Malaysia Melaka (UTeM) for the research grant (PJP/2013/FKE(5D)/S01171) provided for this project. Also to Prof. Dr. Yasutaka Fujimoto from Yokohama National University for the robot simulation software.

References

1. Calanca A, Capisani LM, Ferrara A, Magnani L (2011) MIMO closed loop identification of an industrial robot. IEEE Trans Control Syst Technol 19(5):1214–1224
2. Bonilla I, Mendoza M, Gonzalez-Galvan EJ, Chavez-Olivares C, Loredo-Flores A, Reyes F (2012) Path-tracking maneuvers with industrial robot manipulators using uncalibrated vision and impedance control. IEEE Trans Syst Man Cybern Part C Appl Rev 42(6):1716–1729
3. Bartsch S, Birnschein T, Cordes F, Kuehn D, Kampmann P, Hilljegerdes J, Planthaber S, Roemmermann M, Kirchner F (2010) SpaceClimber: Development of a six-legged climbing robot for space exploration. In: IEEE Proceedings on 2010, 41st international symposium on robotics (ISR) and 2010, 6th German conference on robotics (ROBOTIK), Bremen, pp 1–8
4. Saenz J, Elkmann N, Stuerze T, Kutzner S, Althoff H (2010) Robotic systems for cleaning and inspection of large concrete pipes. In: IEEE Proceedings on 2010, 1st international conference on applied robotics for the power industry (CARPI), Montreal, pp 1–7 (2010)
5. Shukor AZ, Fujimoto Y (2011) Workspace control of biarticular manipulator. In: IEEE Proceedings on 2011, international conference on mechatronics (ICM), pp 415–420
6. Focchi M, Boaventura T, Semini C, Frigerio M, Buchli J, Caldwell DG (2012) Torque-control based compliant actuation of a quadruped robot. In: IEEE Proceedings of 12th international workshop on advanced motion control, IEEE, pp 1–6

7. Salvucci V, Kimura Y, Sehoon Oh, Hori Y (2013) Force maximization of biarticularly actuated manipulators using infinity norm. IEEE/ASME Trans Mechatron 18(3):1080–1089
8. Sehoon Oh, Kimura Y, Hori Y (2010) Force control based on biarticular muscle system and its application to novel robot arm driven by planetary gear system. In: Proceedings on 2010, IEEE/RSJ international conference on intelligent robots and systems (IROS), IEEE, pp 4360–4365
9. Fujimoto Y, Kawamura A (1998) Simulation of an autonomous biped walking robot including environmental force interaction. IEEE Robot Autom Mag 5(2):33–42

Springer
http://www.springer.com/978-981-4585-41-5

The 8th International Conference on Robotic, Vision, Signal Processing & Power Applications
Innovation Excellence Towards Humanistic Technology
Mat Sakim, H.A.; Mustaffa, M.T. (Eds.)
2014, XX, 539 p. 253 illus., 165 illus. in color., Hardcover
ISBN: 978-981-4585-41-5